MedChemComm

Accepted Manuscript

This article can be cited before page numbers have been issued, to do this please use: J. Lan, T. ZHANG, Y. Liu, Y. Zhang, J. Hou, S. Xie, J. Yang, Y. Ding and Z. Cai, *Med. Chem. Commun.*, 2017, DOI: 10.1039/C6MD00586A.

ROYAL SOCIETY OF CHEMISTRY

rsc.li/medchemcomm

View Article Online
DOI: 10.1039/C6MD00586A

Synthesis and evaluation of small molecules bearing a benzyloxy substituent as novel and potent Monoamine Oxidase inhibitors†

Jin-Shuai Lan[1#], Tong Zhang[2#], Yun Liu[1], Yong Zhang[1], Jian-wei Hou[1], Sai-Sai Xie[3], Jing Yang[1], Yue Ding[1*], Zhen-zhen Cai[4*]

1 Experiment Center of Teaching & Learning, Shanghai University of Traditional Chinese Medicine, Shanghai 201203, China;

2 School of Pharmacy, Shanghai University of Traditional Chinese Medicine, Shanghai 201203, China;

3 National Pharmaceutical Engineering Center for Solid Preparation in Chinese Herbal Medicine, Jiangxi University of Traditional Chinese Medicine, Nanchang 330006, China;

4 Experiment Center for Science and Technology, Shanghai University of Traditional Chinese Medicine, Shanghai 201203, China.

* Corresponding author.

* E-mail: zhangtongshutcm@hotmail.com (TZ); dingyue-2001@hotmail.com (YD)

# These authors contributed equally to this work.

†The authors declare no competing interests.

View Article Online
DOI: 10.1039/C6MD00586A

Abstract

A new series of small molecules bearing the benzyloxy substituent have been designed, synthesized and evaluated for *h*MAO inhibitory activity *in vitro*. Most of compounds were potent and selective MAO-B inhibitors, and were weak inhibition on MAO-A. In particular, compounds **9e** (IC_{50} = 0.35 μM) and **10e** (IC_{50} = 0.19 μM) were the most potent MAO-B inhibitors, and exhibited the highest selectivity for MAO-B (**9e**, SI > 285.7-fold and **10e**, SI = 146.8-fold). In addition, the structure-activity relationships for MAO-B inhibition indicated that electron-withdrawing groups in the open small molecules were more suitable for MAO-B inhibition, and substitutions at the benzyloxy of the open small molecules, particularly with the halogen substituted benzyloxy, were more favorable for MAO-B inhibition. Molecular docking studies have been done to explain the potent MAO-B inhibition of the open small molecules. Furthermore, the representative compounds **9e** and **10e** showed low neurotoxicity in SH-SY5Y cells *in vitro*. So the small molecules bearing the benzyloxy substituent could be used to develop promising drug candidates for the therapy of neurodegenerative diseases.

Keywords

Monoamine Oxidase; benzyloxy substituent; neurodegenerative diseases; Molecular docking.

Abbreviations

View Article Online
DOI: 10.1039/C6MD00586A

MAO, Monoamine oxidase; CNS, central nervous system; 5-HT, 5-hydroxy-tryptamine; NE, norepinephrine; DA, dopamine; FAD, flavin adenine dinucleotide; SI, selectivity index; BBB, blood-brain barrier; MTT, methyl thiazolyl tetrazolium.

Introduction

Monoamine oxidase (EC 1.4.3.4; MAO), located in the peripheral tissues and central nervous system (CNS), is a FAD-containing enzyme, which binds tightly to the outer mitochondrial membrane of glial, neuronal and other cells. MAOs could regulate and metabolize biogenic amines by oxidative deamination, such as serotonin, dopamine (DA) and epinephrine.[1]

On account of differences in inhibitor specificity, immunological properties, substrate preference, amino acid sequences and tissue distribution, mammals contain two distinctive MAO enzymes, namely MAO-A and MAO-B.[2-6] The MAO-A preferentially metabolizes epinephrine, norepinephrine, and serotonin, and is selectively inhibited by clorgyline. Whereas the MAO-B is selectively inhibited by selegiline or rasagiline, and specifically deaminates β-phenethylamine.[7-8] With an increasing number of studies in X-ray crystal structures of the two MAOs, information about the pharmacophoric requirements and the selective interactions is useful to design potent and selective MAO inhibitors. The active sites of *h*MAOs are supposed to be the key structural differences because of the different shapes and volume of the inhibitors/substrate binding pockets. The active site of *h*MAO-A is a single hydrophobic cavity, while *h*MAO-B has two distinct cavities: one is the

View Article Online
DOI: 10.1039/C6MD00586A

so-called “substrate cavity”, which is connected to the flavine adenine dinucleotide cofactor (FAD) and the other smaller cavity called “entrance cavity” is located towards the outside of the protein. These cavities of MAOs have narrow pockets, but in *h*MAO-B the Tyr326 and Ile199 residues act as a bottleneck and thus form a gate, which separates the region as two cavities.[9-10]

Since the MAOs could terminate the actions of neurotransmitter amines in the CNS, they are regarded as attractive targets to treat psychiatric and neurological disorders. Selective MAO-A inhibitors are effective in the therapy of depression,[11] while selective MAO-B inhibitors have been applied alone or in combination to treat Alzheimer's and Parkinson's diseases.[12] Thus the specific MAO inhibitors are developed for the treatment of neurological disorder.

Hetero-benzofused derivatives bearing a benzyloxy substituent, for novel MAO-B inhibitors, have been selected as promising scaffolds with potent inhibition.[13-20] These MAO-B inhibitors are related to natural compounds, such as coumarins, indoles, chromones, and chromanones analogues (Fig. 1. compounds **1**-**4**).[13-16] Interestingly, we find that some smaller molecules also exhibit potent MAO-B inhibitory activity, when the heterocycle of hetero-benzofused derivatives is opened (Fig. 1. compounds **5**-**8**).[17-20] Because these MAO-B inhibitors with benzyloxy substituents are substantially similar, we suppose that the simplified substituents on the benzene ring (A) may also have potential MAO-B inhibitory properties, and the different small substituents may affect the MAO-B inhibitory activity. To obtain the smaller MAO-B inhibitors with novel structure, we modify the molecular structure by introducing

View Article Online
DOI: 10.1039/C6MD00586A

different substituents (Br, CHO, and OCH_3) at *meta*-position of the benzene ring (A) (Fig. 2). To further examine the structure–activity relationships (SAR) against MAO, different substitutions (F, Br and CH_3) were introduced to the benzyloxy ring, and the properties on MAO inhibition were examined.

Results and Discussion

Chemistry

The target compounds (**9a–g**, **10a–g** and **11a–g**) were efficiently synthesized as shown in Scheme 1. The commercially available 3-bromophenol (**9**), 3-Hydroxybenzaldehyde (**10**) and 3-methoxyphenol (**11**) were reacted with the appropriate benzyl bromides in the presence of K_2CO_3 to give the target compounds in good yields (85-97%).

Inhibition of *h*MAO activity

For compounds **9a–g**, **10a–g** and **11a–g**, the MAO inhibitory activities were tested with iproniazid as a reference.[21] The corresponding IC_{50} values with MAO and the selectivity ratios (IC_{50} of MAO-A/IC_{50} of MAO-B) were shown in Table 1. It could be seen that most of the tested compounds (except compound **11a-g**) were selective MAO-B inhibitors with IC_{50} values in the low micromole range. Among the synthesized compounds, compound **9e** (IC_{50} = 0.35 μM, SI > 285.7) and compound **10d** (IC_{50} = 0.19 μM, SI = 206.3) were the most potent and selective inhibitors against MAO-B, being about 23.5-fold more and 43.4-fold more active than iproniazid.

Initially, introducing benzyloxy groups to compounds **9**, **10** and **11**, compounds **9a, 10a** and **11a** were synthesized. As shown in Table 1, compound **11a**,

View Article Online
DOI: 10.1039/C6MD00586A

OCH_3-substitution at *meta*-position of the benzene ring (A), exhibited an IC_{50} value of 15.8 μM for MAO-B which was less active than Br-substituted compound **9a** (IC_{50} = 2.73 μM) and CHO-substituted compound **10a** (IC_{50} = 1.96 μM). From this result, it might be concluded that the electron-withdrawing groups at meta-position of the benzene ring (A) was more suitable for MAO-B inhibition.

Then, we thought of introducing substituents with varying positions and electronic properties to benzyloxy substitution to study the possible effects on MAO-B inhibition potency. It was noteworthy that the substituted at the *para*-positions (compounds **9c**, **9e** and **9g**) were more potent than the corresponding *meta*-position (compounds **9b**, **9d** and **9f**). Compared to compound **9a**, compounds **9b-e** bearing electron-withdrawing groups exhibited large enhancement in MAO-B inhibition. However, compounds **9f** and **9g** with an electron-donating group showed a slight increase in MAO-B inhibition. For example, compound **9e** (IC_{50} = 0.35 μM for MAO-B) possessing an electron-withdrawing substituent Br was about 8-fold more active than compound **9a,** while compound **9f** (IC_{50} = 1.98 μM for MAO-B) substituted with CH_3, increased the MAO-B inhibition potency of compound **9a** by 1.4-fold. Furthermore, among compounds **9b-g**, compounds with *para*-substitution of the benzyloxy phenyl ring were more portent for MAO-B inhibition than *meta*-substitution.

Moreover, introducing different substituents to benzyloxy of compound **10a** to study the possible effects on MAO inhibition, compounds **10b–g** were synthesized. Interestingly, the substituted at the *para* positions were more potent than the

View Article Online
DOI: 10.1039/C6MD00586A

corresponding *meta*-position, which was consistent with the compounds **9b–g**. Additionally, compared to compound **10a**, compounds **10f** and **10g** with an electron-donating group showed a slight decrease in MAO-B inhibition.

Overall, these results demonstrated that substitution with a wide variety of benzyloxy side chains of small molecules led to structures with potent MAO-B inhibition. While MAO-A inhibition was very weak and no apparent SARs existed.

Reversibility of *h*MAO-B inhibition

As we know, MAO-B inhibitors could be classified as irreversible and reversible. To examine whether the small molecules bearing a benzyloxy substituent were reversible or irreversible MAO-B inhibitors, the time dependencies of inhibition was evaluated.[14] Compounds **9e** and **10e** were selected as representative inhibitors since they displayed the most potent MAO-B inhibitory activity. For a reversible inhibitor, the MAO-B activity would be almost the same, when the enzyme was preincubated with a reversible inhibitor over different time periods. In contrast, for an irreversible inhibitor the MAO-B activity would show a time-dependent reduction. Compounds **9e** and **10e** were preincubated with MAO-B over different time periods (0-60 min) at a concentration of twofold IC_{50}. As shown in Fig. 3, we could observe that MAO-B activities were almost the same (Compound **9e:** 44.8% at 0 min, 44.9% at 15 min, 48.6% at 30 min and 49.2% at 60 min; Compound **10e:** 46.4% at 0 min, 45.8% at 15 min, 49.9% at 30 min and 49.5% at 60 min), and the result demonstrated that compounds **9e** and **10e** were not time-dependent inhibitors of MAO-B. So these experiments clearly indicated that the small molecules bearing a benzyloxy

View Article Online
DOI: 10.1039/C6MD00586A

substituent were reversible MAO-B inhibitors.

Kinetic study of *h*MAO-B inhibition

Compound **9e** was also used to further investigate the mode of MAO-B inhibition. The type of MAO-B inhibition was determined by Michaelis-Menten kinetic experiments.[22] The catalytic rates were measured at five different *p*-tyramine concentrations (50-500 μM), and each plot was constructed at four different concentrations of compound **10e** (0, 0.095, 0.19 and 0.38 μM). The overlaid reciprocal Lineweaver-Burk plots (Fig. 4) showed that the plots for different concentrations of compound **9e** were linear and intersected at the *y*-axis. This pattern indicated that compound **9e** was a competitive MAO-B inhibitor, and these results further proved that the small molecules bearing a benzyloxy substituent were reversible MAO-B inhibitors.

Molecular modeling studies

In order to explain the difference in MAO-B inhibiton, we have carried out a structure-based molecular modeling study using *h*MAOs cocrystals deposited into the PDB. Crystallographic structures of MAO-B (PDB code 2V61) was used to dock the derivatives under study.[17] And molecular docking study was performed using software package MOE 2008.10.[23] According to the inhibition results, compounds **9e**, **10e** and **11e** with different small substituents (Br, CHO, and OCH_3) at *meta*-position of the benzene ring (A) was selected as a typical ligand. The 3D and 2D pictures of binding were illustrated in Fig. 5. As shown in Fig. 5A and 5B, compound **9e** located in the well-known binding pocket of MAO-B,[24] with the Br-substituted benzene ring (A)

View Article Online
DOI: 10.1039/C6MD00586A

interacting with Tyr 398 via an aromatic π-π stacking interactions at bottom of the substrate cavity; The Br-substituted benzyl group occupied the entrance cavity via a π-πinteraction with Tyr 326. From Fig. 5C and 5D, compound **10e**, with the CHO-substituted benzene ring (A), not only had an aromatic π-π stacking interactions with Tyr 398, but also had a hydrogen bond interaction with Tyr 188 at bottom of the substrate cavity; The Br-substituted benzyl group occupied the entrance cavity which was a hydrophobic subpocket existing only in the MAO-B isoform and constituted by Leu 171, Ile 316, Tyr 326, Ile 199, Phe 99, Pro 104 and Phe 168. However, no interaction between the ligands **11e** with the OCH_3-substituted benzene ring (A) and the MAO-B was observed in Fig. 5E and 5F. So these results might explain why the MAO-B inhibitory activities of compounds **9e** and **10e** were more potent than that of compound **11e**, and the reason could be ascribed to the different interaction between compounds and the MAO-B. Moreover, the modelling studies between compound **10e** and standard compound 7-((3-chlorobenzyl)oxy)-4-((methylamino)methyl) -coumarin(Claudia Binda, *J Med Chem.* **2007**, *50*, 5848-5852.) were compared in supporting information.

Cells toxicity

Based on the screening results above, compounds **9e** and **10e** as the most potent inhibitors against MAO-B were selected to further examine the potential toxicity effect on the SH-SY5Y cells.[25] After incubating the cells with compound **9e** or **10e** for 48 h, the cell viability was determined by the 3-(4,5-dimethylthiazol-2-yl)-2,5-diphenyltetrazolium (MTT) assay. As shown in the Fig. 6, the result revealed

View Article Online
DOI: 10.1039/C6MD00586A

that compounds **9e** and **10e** at 3-50 μM did not have neurotoxicity. This suggested that compounds **9e** and **10e** might be used to develop promising drug candidates for the therapy of neurodegenerative diseases.

Prediction of BBB penetration of compounds 9a-g, 10a-g and 11a-g

High pharmacological activity and low toxicological effects are not enough for a compound to become a drug candidate. Molecules should meet the limiting terms of Lipinski's rules: molecular weight (MW) less than 500, the number of hydrogen bond acceptor atoms (HBA) less than 10, the number of hydrogen bond donor atoms (HBD) less than 5, the calculated logarithm of the octanol-water partition coefficient (Clog P) less than 5, and the small polar surface area less than 90 $Å^2$. With the aim of developing the CNS drugs, the ability of compounds to cross the blood-brain barrier (BBB) is very important.[26] The log BB is calculated as the following equation: log BB = 0.0148 × PSA + 0.152 × Clog P + 0.139.[27] Calculated log BB for potential applications in brains and defined by the restrictive terms of Lipinski's rules, as shown in Table 2, compounds **9a-g**, **10a-g** and **11a-g** satisfied possible brain penetration and drug-like standards.

Conclusions

In conclusion, we have synthesized a series of small molecules bearing the benzyloxy substituent and evaluated their MAO inhibitory activity and toxicity *in vitro*. The results showed that most of the studied compounds were remarkably competitive and reversible MAO-B inhibitors rather than of MAO-A. The SAR of synthesized compounds showed the electron-withdrawing groups at meta-position of

View Article Online
DOI: 10.1039/C6MD00586A

the benzene ring (A) were more suitable for MAO-B inhibition; halogen substituents on the benzyloxy ring further increased MAO-B inhibition. So different electron-withdrawing groups will be introduced at different position of the benzene ring (A) and the MAO-B inhibition will be tested, which is on further study. Moreover, molecular docking studies of the **9e** and **10e** suggested that the potent MAO-B inhibition might be ascribed to the π-π stacking/cation–π interactions and the larger set of residues interacting with MAO-B. Due to the possible BBB permeability and low neurotoxicity in SH-SY5Y cells *in vitro*, these compounds could be used to develop promising drug candidates for the therapy of neurodegenerative diseases.

Experimental Section

Materials and Methods

All chemicals (reagent grade) used were purchased from Sino pharm Chemical Reagent Co., Ltd. (China). Reaction progress was monitored using analytical thin layer chromatography (TLC) on precoated silica gel GF254 (Qingdao Haiyang Chemical Plant, Qing-Dao, China) plates and the spots were detected under UV light (254 nm). ^{1}H NMR and ^{13}C NMR spectra were measured on a BRUKER AVANCE III spectrometer at 25°C and referenced to TMS. Chemical shifts are reported in ppm (δ) using the residual solvent line as internal standard. Splitting patterns are designed as s, singlet; d, doublet; t, triplet; m, multiplet. The purity of all compounds was confirmed to be higher than 95% through analytical HPLC performed with Agilent 1200 HPLC System, photodiode array detector (DAD), 55% (v/v) of CH_3OH gradient, flow rate: 1.0 mL /min. Mass spectra were obtained on a MS Agilent 1100 Series LC/MSD Trap

View Article Online
DOI: 10.1039/C6MD00586A

mass spectrometer (ESI-MS).

General Procedure for the Preparation of compounds 9a–g, 10a–g and 11a–g.

Compounds **9**, **10** or **11** (1.85 mmol) was suspended in acetonitrile (15 mL) containing K_2CO_3 (3.70 mmol). The reaction was treated with an appropriately substituted arylalkyl bromide (2.04 mmol) and heated under reflux for 12 h. The reaction progress was monitored using *silica gel* TLC with hexanes/EtOAc as mobile phase. Upon completion, the acetonitrile was evaporated *in vacuo* and the mixture was then poured into water, which was extracted with 3 × 200 mL of EtOAc, washed with brine, dried over anhydrous Na_2SO_4 and purified by chromatography (hexanes /EtOAc) on *silica gel.*

1-(benzyloxy)-3-bromobenzene (**9a**)

Yield 89%; light yellow oil; ESI/MS *m/z*: 264.1 $[M+H]^+$; ^{1}H-NMR (400 MHz, $CDCl_3$): δ 7.45–7.38 (m, 4H), 7.37–7.31 (m, 1H), 7.18–7.07 (m, 3H), 6.95-6.87 (m, *J* = 8.0, 2.4, 1.2 Hz, 1H), 5.05 (s, 2H). ^{13}C-NMR (100 MHz, $CDCl_3$): δ 159.57, 136.42, 130.59, 128.68, 128.18, 127.51, 124.10, 122.84, 118.22, 113.86, 70.24.

1-bromo-3-((3-fluorobenzyl)oxy)benzene (**9b**)

Yield 92%; light yellow oil; ESI/MS *m/z*: 282.1 $[M+H]^+$; ^{1}H NMR (400 MHz, $CDCl_3$) δ 7.36-7.25 (m, 1H), 7.20 –7.09 (m, 5H), 7.03-6.95 (m, 1H), 6.89-6.81 (m, 1H), 5.04 (s, 2H). ^{13}C-NMR (100 MHz, CDCl3) δ 162.93(d, $^1J_{CF}$= 287.43 Hz), 159.24, 139.01(d, $^3J_{CF}$ = 8.27 Hz), 130.64, 130.22(d, $^3J_{CF}$ = 8.48 Hz), 124.35, 122.88, 122.71, 118.21, 115.01 (d, $^2J_{CF}$ = 21.68 Hz), 114.23 (d, $^2J_{CF}$ = 22.25 Hz), 113.80, 69.37.

1-bromo-3-((4-fluorobenzyl)oxy)benzene (**9c**)

View Article Online
DOI: 10.1039/C6MD00586A

Yield 93%; light yellow oil; ESI/MS *m/z*: 282.1 $[M+H]^+$; ^{1}H NMR (400 MHz, $CDCl_3$) δ 7.43–7.35 (m, 2H), 7.18–7.03 (m, 5H), 6.89-6.79 (m, 1H), 5.00 (s, 2H). ^{13}C-NMR (100 MHz, $CDCl_3$) δ 162.62(d, $^1J_{CF}$= 245.43 Hz), 159.37, 132.18, 132.15, 130.62, 129.38(d, $^3J_{CF}$ = 8.36 Hz), 124.24, 122.87, 118.19, 115.59, 115.59(d, $^2J_{CF}$ = 21.59 Hz), 113.83, 69.56.

1-bromo-3-((3-bromobenzyl)oxy)benzene(9d)

Yield 89%; light yellow oil; ESI/MS *m/z*: 343.0 $[M+H]^+$; ^{1}H NMR (400 MHz, $CDCl_3$) δ 7.58 (s, 1H), 7.47 (d, *J* = 7.9 Hz, 1H), 7.34 (d, *J* = 7.7 Hz, 1H), 7.29 – 7.23 (m, 1H), 7.18 – 7.08 (m, 3H), 6.89-6.80 (m, 1H), 5.01 (s, 2H). ^{13}C-NMR (100 MHz, $CDCl_3$) δ 159.22, 138.73, 131.23, 130.66, 130.35, 130.22, 125.84, 124.39, 122.90, 122.76, 118.21, 113.76, 69.28.

1-bromo-3-((4-bromobenzyl)oxy)benzene (9e)

Yield 90%; light yellow oil; ESI/MS *m/z*: 343.1 $[M+H]^+$; ^{1}H NMR (400 MHz, DMSO-d6) δ 7.59 (d, *J* = 8.2 Hz, 2H), 7.40 (d, *J* = 8.2 Hz, 2H), 7.28 –7.20 (m, 2H), 7.14 (d, *J* = 7.9 Hz, 1H), 7.02-6.95 (m, 1H), 5.11 (s, 2H). ^{13}C NMR (101 MHz, DMSO-d6) δ 159.58, 136.55, 131.86, 131.86, 131.69, 130.30, 130.30, 124.23, 122.57, 121.55, 118.16, 114.80, 69.16.

1-bromo-3-((3-methylbenzyl)oxy)benzene (9f)

Yield 87%; light yellow oil; ESI/MS *m/z*: 278.2 $[M+H]^+$; ^{1}H NMR (400 MHz, $CDCl_3$) δ 7.29 (t, *J* = 7.5 Hz, 1H), 7.25–7.20 (m, 2H), 7.18 – 7.08 (m, 4H), 6.91-6.86 (m, 1H), 5.00 (d, *J* = 6.0 Hz, 2H), 2.38 (s, 3H). ^{13}C-NMR (100 MHz, $CDCl_3$) δ 159.63, 138.39,

View Article Online
DOI: 10.1039/C6MD00586A

136.31, 130.57, 128.95, 128.57, 128.27, 124.63, 124.04, 122.83, 118.21, 113.83, 70.31, 21.43.

1-bromo-3-((4-methylbenzyl)oxy)benzene (9g)

Yield 86%; light yellow oil; ESI/MS *m/z*: 278.2 $[M+H]^+$; ^{1}H NMR (400 MHz, $CDCl_3$) δ 7.31 (d, *J* = 8.0 Hz, 2H), 7.21 (d, *J* = 7.8 Hz, 2H), 7.17–7.05 (m, 3H), 6.90-6.83 (m, 1H), 5.00 (s, 2H), 2.37 (s, 3H). ^{13}C-NMR (100 MHz, $CDCl_3$) δ 159.64, 138.00, 133.36, 130.55, 129.35, 129.35, 127.66, 127.66, 123.99, 122.81, 118.21, 113.87, 70.18, 21.22.

3-(benzyloxy)benzaldehyde (**10a**)

Yield 88%; light yellow oil; ESI/MS *m/z*: 213.2 $[M+H]^+$; ^{1}H NMR (400 MHz, $CDCl_3$) δ 9.98 (s, 1H), 7.50 – 7.32 (m, 8H), 7.26-6.17 (m, 1H), 5.13 (s, 2H). ^{13}C-NMR (100 MHz, $CDCl_3$) δ 192.07, 159.35, 137.86, 136.33, 130.13, 128.70, 128.70, 128.22, 127.55, 127.55, 123.69, 122.21, 113.32, 70.26.

3-((3-fluorobenzyl)oxy)benzaldehyde (10b)

Yield 93%; light yellow oil; ESI/MS *m/z*: 231.2 $[M+H]^+$; ^{1}H NMR (400 MHz, $CDCl_3$) δ 9.98 (s, 1H), 7.52–7.44 (m, 3H), 7.36-7.24 (m, 1H), 7.27–7.14 (m, 3H), 7.03 (td, *J* = 8.3, 2.4 Hz, 1H), 5.12 (s, 2H). ^{13}C-NMR (100 MHz, $CDCl_3$) δ 191.97, 163.02(d, $^1J_{CF}$= 245.48 Hz), 159.05, 138.93 (d, $^3J_{CF}$ = 7.83 Hz), 137.89, 130.30, 130.22, 123.99, 122.79, 122.17, 115.06(d, $^2J_{CF}$ = 21.32 Hz), 114.27(d, $^2J_{CF}$ = 22.14 Hz), 113.14, 69.38.

3-((4-fluorobenzyl)oxy)benzaldehyde (10c)

View Article Online
DOI: 10.1039/C6MD00586A

Yield 90%; light yellow oil; ESI/MS *m/z*: 231.2 $[M+H]^+$; ^{1}H NMR (400 MHz, $CDCl_3$) δ 9.98 (s, 1H), 7.50–7.45 (m, 3H), 7.45 – 7.39 (m, 2H), 7.27–7.22 (m, 1H), 7.12–7.06 (m, 2H), 5.08 (s, 2H). ^{13}C-NMR (100 MHz, $CDCl_3$) δ 192.02, 162.64(d, $^1J_{CF}$= 245.58 Hz), 159.17, 137.87, 132.08, 130.18, 129.43, 129.43(d, $^3J_{CF}$ = 8.27 Hz), 123.92, 122.22, 115.62, 115.62(d, $^2J_{CF}$ = 21.84 Hz), 113.11, 69.57.

3-((3-bromobenzyl)oxy)benzaldehyde (10d)

Yield 90%; light yellow oil; ESI/MS *m/z*: 292.1 $[M+H]^+$; ^{1}H NMR (400 MHz, $CDCl_3$) δ 9.95 (s, 1H), 7.59 (s, 1H), 7.49–7.45 (m, 2H), 7.45–7.42 (m, 2H), 7.34 (d, *J* = 7.7 Hz, 1H), 7.25–7.20 (m, 2H), 5.06 (s, 2H). ^{13}C-NMR (100 MHz, $CDCl_3$) δ 191.95, 159.03, 138.65, 137.90, 131.28, 130.39, 130.24, 130.24, 125.90, 124.01, 122.79, 122.14, 113.15, 69.29.

3-((4-bromobenzyl)oxy)benzaldehyde (10e)

Yield 91%; light yellow oil; ESI/MS *m/z*: 292.1 $[M+H]^+$; ^{1}H NMR (400 MHz, DMSO-d6) δ 9.98 (s, 1H), 7.61 (s, 1H), 7.50–7.47 (m, 2H), 7.45–7.41 (m, 2H), 7.35 (d, *J* = 7.7 Hz, 1H), 7.26–7.21 (m, 2H), 5.21 (s, 2H). ^{13}C NMR (100 MHz, DMSO-d6) δ 193.35, 159.09, 139.97, 138.15, 131.25, 131.17, 130.94, 130.72, 130.27, 127.09, 123.43, 122.15, 114.38, 68.95.

3-((3-methylbenzyl)oxy)benzaldehyde (10f)

Yield 89%; light yellow oil; ESI/MS *m/z*: 227.2 $[M+H]^+$; ^{1}H NMR (400 MHz, $CDCl_3$) δ 9.98 (s, 1H), 7.51–7.45 (m, 3H), 7.30–7.22 (m, 4H), 7.16 (d, *J* = 7.3 Hz, 1H), 5.09 (s, 2H), 2.39 (s, 3H). ^{13}C-NMR (100 MHz, $CDCl_3$) δ 192.10, 159.41,

View Article Online
DOI: 10.1039/C6MD00586A

138.43, 137.86, 136.23, 130.12, 129.00, 128.60, 128.32, 124.68, 123.62, 122.18, 113.36, 70.33, 21.43.

3-((4-methylbenzyl)oxy)benzaldehyde (10g)

Yield 91%; light yellow oil; ESI/MS *m/z*: 227.1 $[M+H]^+$; ^{1}H NMR (400 MHz, $CDCl_3$) δ 9.97 (s, 1H), 7.51–7.43 (m, 3H), 7.34 (d, *J* = 8.0 Hz, 2H), 7.27–7.19 (m, 3H), 5.09 (s, 2H), 2.37 (s, 3H). ^{13}C-NMR (100 MHz, $CDCl_3$) δ 192.10, 159.41, 138.05, 137.84, 133.29, 130.10, 130.10, 129.38, 129.38, 127.71, 123.57, 122.23, 113.37, 70.21, 21.22.

1-(benzyloxy)-3-methoxybenzene (11a)

Yield 91%; light yellow oil; ESI/MS *m/z*: 215.2 $[M+H]^+$; ^{1}H NMR (400 MHz, $CDCl_3$) δ 7.60 (s, 1H), 7.46 (d, *J* = 7.9 Hz, 1H), 7.35 (d, *J* = 7.7 Hz, 1H), 7.29 –7.16 (m, 3H), 6.56-6.43 (m, 3H), 5.02 (s, 2H), 3.80 (s, 3H). ^{13}C-NMR (100 MHz, $CDCl_3$) δ 160.91, 159.75, 139.36, 131.03, 130.38, 130.15, 130.00, 125.88, 122.70, 106.90, 106.87, 101.44, 69.13, 55.31.

1-fluoro-3-((3-methoxyphenoxy)methyl)benzene (11b)

Yield 93%; light yellow oil; ESI/MS *m/z*: 233.2 $[M+H]^+$; 1H NMR (400 MHz, $CDCl_3$) δ 7.60 (s, 1H), 7.46 (d, *J* = 7.9 Hz, 1H), 7.35 (d, *J* = 7.7 Hz, 1H), 7.29–7.16 (m, 2H), 6.56-6.41 (m, 3H), 5.02 (s, 2H), 3.80 (s, 3H). ^{13}C-NMR (100 MHz, $CDCl_3$) δ 163.02(d, $^1J_{CF}$= 245.35 Hz), 160.91, 159.78, 139.65(d, $^3J_{CF}$= 8.27 Hz), 130.13 (d, $^3J_{CF}$= 8.24 Hz), 129.99, 122.76, 114.80(d, $^2J_{CF}$= 21.33 Hz), 114.26(d, $^2J_{CF}$= 22.26 Hz), 106.93, 106.81, 101.44, 69.21, 55.30.

1-((4-fluorobenzyl)oxy)-3-methoxybenzene (11c)

View Article Online
DOI: 10.1039/C6MD00586A

Yield 91%; light yellow oil; ESI/MS *m/z*: 233.2 $[M+H]^+$; ^{1}H NMR (400 MHz, $CDCl_3$) δ 7.45–7.36 (m, 2H), 7.23–7.16 (m, 1H), 7.12–7.02 (m, 2H), 6.60–6.50 (m, 3H), 5.01 (s, 2H), 3.79 (s, 3H). ^{13}C-NMR (100 MHz, $CDCl_3$) δ 162.54(d, $^1J_{CF}$= 245.19 Hz), 160.89, 159.89, 132.73, 129.96, 129.38, 129.38(d, $^3J_{CF}$= 8.95 Hz), 115.50, 115.50(d, $^3J_{CF}$= 22.11 Hz), 106.94, 106.71, 101.43, 69.37, 55.29.

1-bromo-3-((3-methoxyphenoxy)methyl)benzene (11d)

Yield 90%; light yellow oil; ESI/MS *m/z*: 294.1 $[M+H]^+$; ^{1}H NMR (400 MHz, $CDCl_3$) δ 7.45 (m, 2H), 7.42 –7.37 (m, 2H), 7.20 (t, *J* = 8.1 Hz, 1H), 6.62–6.51 (m, 3H), 5.06 (s, 2H), 3.80 (s, 3H). ^{13}C-NMR (100 MHz, $CDCl_3$) δ 160.88, 160.10, 137.01, 129.93, 128.62, 128.62, 128.00, 127.55, 127.55, 106.99, 106.64, 101.43, 70.08, 55.30.

1-((4-bromobenzyl)oxy)-3-methoxybenzene (11e)

Yield 94%; light yellow oil; ESI/MS *m/z*: 294.1 $[M+H]^+$; ^{1}H NMR (400 MHz, $CDCl_3$) δ 7.58 (d, *J* = 8.3 Hz, 2H), 7.40 (d, *J* = 8.3 Hz, 2H), 7.18 (t, *J* = 8.1 Hz, 1H), 6.60–6.54 (m, 2H), 6.53 (dd, *J* = 8.2, 2.1 Hz, 1H), 5.07 (s, 2H), 3.72 (s, 3H). ^{13}C NMR (100 MHz, DMSO-d6) δ 160.97, 159.83, 137.07, 131.81, 131.81, 130.46, 130.22, 130.22, 121.35, 107.46, 107.04, 101.60, 68.84, 55.56.

1-methoxy-3-((3-methylbenzyl)oxy)benzene (11f)

Yield 91%; light yellow oil; ESI/MS *m/z*: 229.2 $[M+H]^+$; ^{1}H NMR (400 MHz, $CDCl_3$) δ 7.36–7.13 (m, 5H), 6.59-6.47 (m, 3H), 5.04 (s, 2H), 3.82 (s, 3H), 2.41 (s, 3H). ^{13}C NMR (100 MHz, $CDCl_3$) δ 160.87, 160.16, 138.30, 136.89, 129.90, 128.77, 128.51, 128.31, 124.67, 106.95, 106.60, 101.40, 70.14, 55.29, 21.43.

1-methoxy-3-((4-methylbenzyl)oxy)benzene (11g)

View Article Online
DOI: 10.1039/C6MD00586A

Yield 91%; light yellow oil; ESI/MS *m/z*: 229.3 $[M+H]^+$; ^1H NMR (400 MHz, $CDCl_3$) δ 7.36 (d, *J* = 8.0 Hz, 2H), 7.22 (t, *J* = 8.2 Hz, 3H), 6.67 – 6.52 (m, 3H), 5.04 (s, 2H), 3.82 (s, 3H), 2.40 (s, 3H). ^{13}C NMR (100 MHz, $CDCl_3$) δ 160.85, 160.16, 137.76, 133.94, 129.88, 129.28, 129.28, 129.28, 129.28, 106.98, 106.55, 101.40, 69.99, 55.28, 21.21.

Acknowledgments

This work was supported by the programs of the National Natural Science Foundation of China [Grant No.81274200, 81403175]; Youth Talent Sail Plan from Shanghai Committee of Science and Technology [Grant No. 14YF1411300]; Project from Shanghai Municipal Commission of Health and Family planning [Grant No. 20134Y053] and Research Fund for the Docoral Program of Shanghai [Grant No. 13401900301].

Conflicts of Interest

The authors declare no conflict of interest.

References

1. Tipton, K. *Cell. Biochem. Funct.* **1986**, *4*, 79-87.

2. Bach, A.; Lan, N. C.; Johnson, D. L.; Abell, C. W.; Bembenek, M. E.; Kwan, S.-W.; Seeburg, P. H.; Shih, J. C. *Proc. Natl. Acad. Sci. USA.* **1988**, *85*, 4934-4938.

3. Wouters, J. *Curr. Med. Chem.* **1998**, *5*, 137-162.

4. Grimsby, J.; Lan, N. C.; Neve, R.; Chen, K.; Shih, J. C. *J. Neurochem.* **1990**, *55*, 1166-1169.

5. Kalgutkar, A. S.; Castagnoli, N.; Testa, B. *Med. Res. Rev.* **1995**, *15*, 325-388.

View Article Online
DOI: 10.1039/C6MD00586A

6. Geha, R. M.; Rebrin, I.; Chen, K.; Shih, J. C. *J. Biol. Chem.* **2001**, *276*, 9877-9882.

7. Ma, J.; Yoshimura, M.; Yamashita, E.; Nakagawa, A.; Ito, A.; Tsukihara, T. *J. Mol. Biol*. **2004**, *338*,103-114.

8. Weyler, W.; Hsu, Y.-P. P.; Breakafield, X. O. *Pharmacol. Ther.* **1990**, *47*, 391-417.

9. Binda, C.; Li, M.; Hubálek, F.; Restelli, N.; Edmondson, D. E.; Mattevi, A. *Proc. Natl. Acad. Sci. U.S.A.* **2003**, *100*, 9750-9755.

10. Ma, J.; Yoshimura, M.; Yamashita, E.; Nakagawa, A.; Ito, A.; Tsukihara, T. *J. Mol. Biol.* **2004**, *338*, 103-114.

11. Chen, J. J.; D. Swope, M.; Dashtipour, K. *Clin. Ther*. **2007**, *29*, 1825-1849.

12. Pacher, P.; Kecskemeti, V. *Curr. Med. Chem.* **2004**, *11*, 925-943.

13. Gnerre C.; Catto M.; Leonetti F.; Weber, P.; Carrupt, P.-A.; Altomare, C.; Carotti, A.; Testa, B. *J. Med. Chem.* **2000**, *43*, 4747-4758.

14. Legoabe, L. J.; Petzer, A.; Petzer, J. P. Bioorg Chem. **2012**, *45*, 1-11.

15. Lan, JS.; Xie, SS.; Huang, M.; Hu, YJ.; Kong LY.; Wang XB. *Med. Chem. Commun.* **2015**, *6*, 1293-1302.

16. Perez, V.; Unzeta, M. *Neurochem Int*. **2003**, *42*, 221-229.

17. Binda, C.; Wang, J.; Pisani, L.; Caccia, C.; Carotti, A.; Salvati, P.; Edmondson, DE.; Mattevi, A. *J Med Chem.* **2007**, *50*, 5848-5852.

18. Manley-King, CI.; Bergh, JJ.; Petzer, JP. *Bioorg Chem.* **2012**, *40*,114-124.

19. Legoabe, LJ.; Petzer, A.; Petzer, JP. *Bioorg Med Chem Lett*. **2012**, *22*, 5480-5484.

View Article Online
DOI: 10.1039/C6MD00586A

20. Wang, ZM.; Li, XM.; Xu, W.; Li, F.; Wang, J.; Kong, LY.; Wang XB. *Med. Chem. Commun.* **2015**, *6*, 2146-2157.

21. Santana, L.; González-Díaz, H.; Quezada, E. a.; Uriarte, E.; Yáñez, M.; Vina, D.; Orallo, F. *J. Med. Chem.* **2008**, *51*, 6740-6751.

22. Tzvetkov, N. T.; Hinz, S.; Küppers, P.; Gastreich, M.; Müller, C. E. *J Med Chem.* **2014**, *15*, 6679-6703.

23. Muzammil, S.; Armstrong, A.; Kang, L.; Jakalian, A.; Bonneau, P.; Schmelmer, V.; Amzel, L.; Freire, E. *J Virol.* **2007**, *81*, 5144-5154.

24. Binda, C.; Hubalek, F.; Li, M.; Herzig, Y.; Sterling, J.; Edmondson, D. E.; Mattevi, A. *J. Med. Chem.* **2004**, *47*, 1767-1774.

25. Lu, C.; Zhou, Q.; Yan, J.; Du, Z.; Huang, L.; Li, X. *Eur. J. Med. Chem.* **2013**, *62*, 745-753.

26. Pardridge, W. M. *Alzheimers Dement.* **2009**, *5*, 427-432.

27. Brayamer, J. J.; DeToma, A. S.; Choi, J.-S.; Ko, K. S.; Lim, M. H. *Int J Alzheimers Dis*. **2011**, *2011*, 623051-623059.

View Article Online
DOI: 10.1039/C6MD00586A

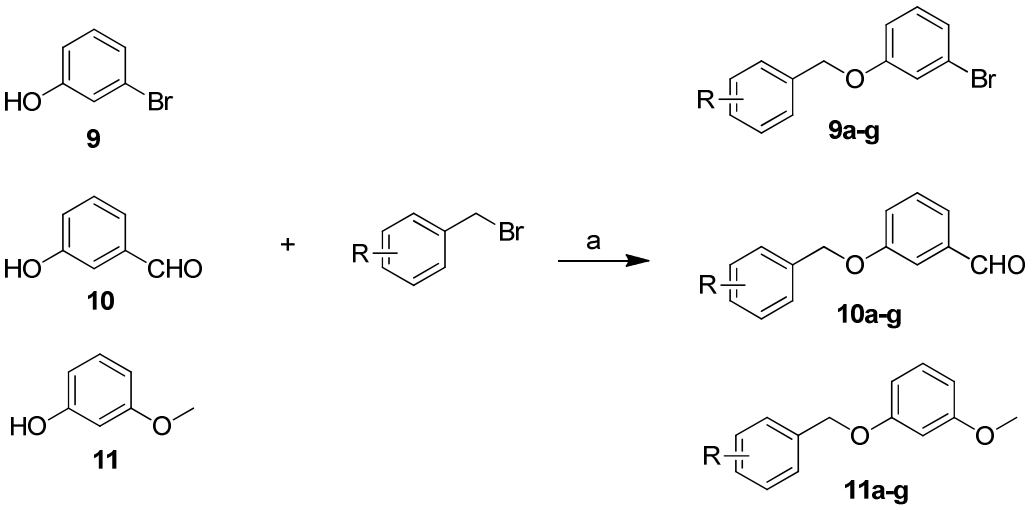

Scheme 1 Syntheses of target compounds **9a–g**, **10a–g** and **11a–g**. Reagents and conditions: (a) K_2CO_3, CH_3CN, reflux, 12 h.

View Article Online
DOI: 10.1039/C6MD00586A

Table 1.

*h*MAO inhibitory activities of the synthesized compounds.

Compounds	R	MAO-A inhibition (%)[a]	MAO-B IC_{50} (μM)[b]	Selectivity Index[c]
9a	-	23	2.73 ± 0.08	>36.6
9b	3-F	37	1.06 ± 0.18	>94.3
9c	4-F	31	0.58 ± 0.12	>172.4
9d	3-Br	27	0.76 ± 0.03	>131.6
9e	4-Br	30	0.35 ± 0.06	>285.7
9f	3-CH_3	43	1.98 ± 0.09	>50.5
9g	4-CH_3	24	1.53 ± 0.06	>65.4
10a	-	45.6 ± 0.87 μM[b]	1.96 ± 0.11	23.3
10b	3-F	64.2 ± 0.59 μM	1.21 ± 0.08	53.1
10c	4-F	42.5 ± 1.06 μM	0.93 ± 0.05	45.7
10d	3-Br	28.2 ± 0.85 μM	0.53 ± 0.04	53.2
10e	4-Br	27.9 ± 0.49 μM	0.19 ± 0.07	146.8
10f	3-CH_3	51.6 ± 0.53 μM	2.91 ± 0.08	17.7
10g	4-CH_3	64.8 ± 0.73 μM	2.53 ± 0.16	25.6
11a	-	25	15.8 ± 0.23	>6.3
11b	3-F	19	12.3 ± 0.79	>8.1
11c	4-F	22	15.6 ± 0.28	>6.4
11d	3-Br	22	19.3 ± 0.51	>5.2
11e	4-Br	25	8.63 ± 0.24	>11.6
11f	3-CH_3	23	10.9 ± 0.17	>9.2
11g	4-CH_3	26	14.6 ± 0.35	>6.8
Iproniazid	-	6.78 ± 0.35 μM	8.24 ± 0.18	0.82

[a] Test concentration is 100 μM.

[b] IC_{50}: 50% inhibitory concentration (means ± SEM of three experiments).

[c] Selectivity Index = IC_{50} (MAO-A)/IC_{50} (MAO-B).

View Article Online
DOI: 10.1039/C6MD00586A

Table 2

Physical properties of compounds **9a-g**, **10a-g** and **11a-g**.

Compounds	MW [a]	Clog P [a]	HBA [a]	HBD [a]	PAS [a]	Log BB [a]
9a	261.99	4.832	1	0	9.23	1.010
9b	279.99	4.975	1	0	9.23	1.031
9c	279.99	4.975	1	0	9.23	1.031
9d	339.91	5.695	1	0	9.23	1.141
9e	339.91	5.695	1	0	9.23	1.141
9f	276.02	5.311	1	0	9.23	0.953
9g	276.02	5.311	1	0	9.23	0.953
10a	212.08	3.546	2	0	26.30	1.067
10b	230.07	3.690	2	0	26.30	1.089
10c	230.07	3.690	2	0	26.30	1.089
10d	289.99	4.410	2	0	26.30	1.199
10e	289.99	4.410	2	0	26.30	1.199
10f	226.10	4.046	2	0	26.30	1.143
10g	226.10	4.046	2	0	26.30	1.143
11a	214.10	3.918	2	0	18.46	0.878
11b	232.09	4.061	2	0	18.46	1.029
11c	232.09	4.061	2	0	18.46	1.029
11d	292.01	4.781	2	0	18.46	1.139
11e	292.01	4.781	2	0	18.46	1.139
11f	228.12	4.417	2	0	18.46	1.084
11g	228.12	4.417	2	0	18.46	1.084
Rules	≤450	≤5.0	≤10	≤5	≤90	≥-1.0

[a] MW: molecular weight; C log P: calculated logarithm of the octanol-water partition coefficient; HBA: hydrogen-bond acceptor atoms; HBD: hydrogen-bond donor atoms; PSA: polar surface area; log BB = 0.0148 × PAS + 0.152 × Clog P + 0.139.

View Article Online
DOI: 10.1039/C6MD00586A

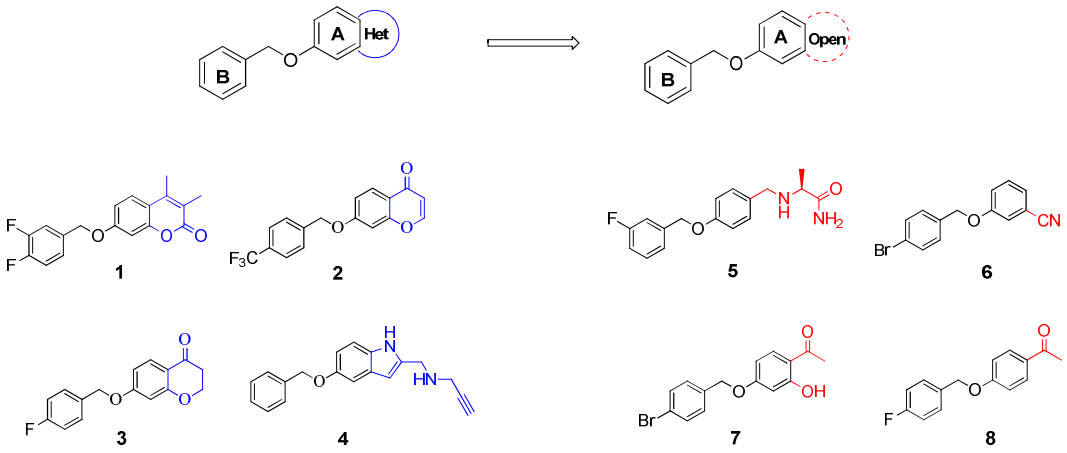

Figure 1. Structures of known MAO inhibitors bearing a benzyloxy substituent.

View Article Online
DOI: 10.1039/C6MD00586A

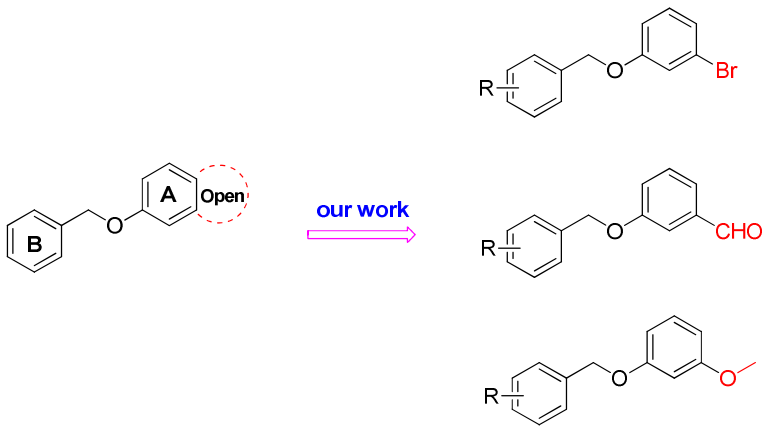

Figure 2. Design strategy for the novel series of heterocycle-opened derivatives as MAO-B inhibitors.

View Article Online
DOI: 10.1039/C6MD00586A

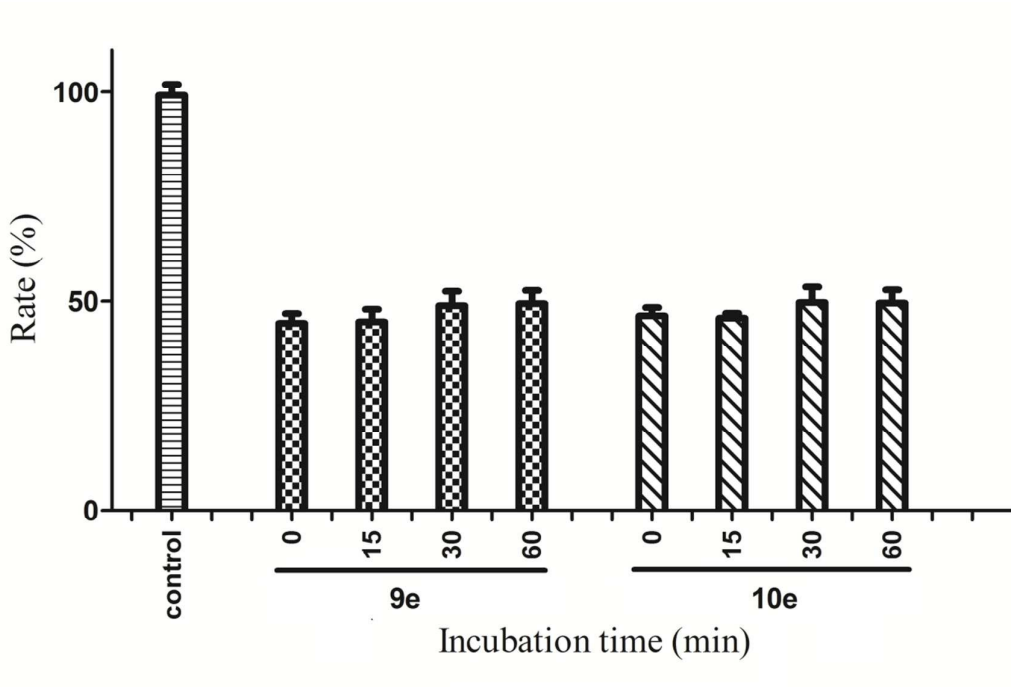

Figure 3. The time-dependent inhibition of *h*MAO-B by compounds **9e** and **10e**. Compound was preincubated for various periods of time (0-60 min) with *h*MAO-B at concentrations equal to twofold the IC_{50} values for the inhibition of the enzyme. After dilution to concentrations equal to the IC_{50}, the inhibitory rates were recorded.

View Article Online
DOI: 10.1039/C6MD00586A

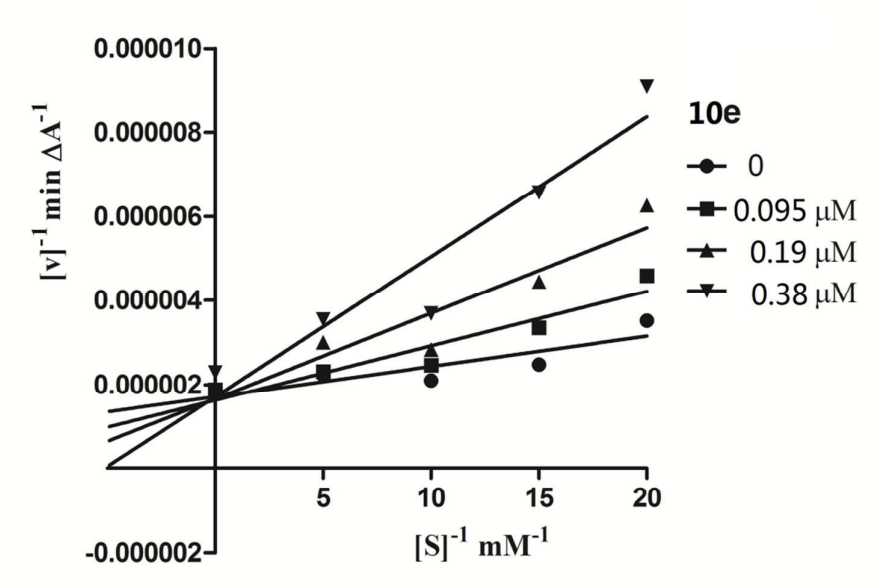

Figure 4. Kinetic study on the mechanism of *h*MAO-B inhibition by compound **10e**. Overlaid Lineweaver-Burk reciprocal plots of MAO-B initial velocity at increasing substrate concentration (50–500 μM) in the absence of inhibitor and in the presence of **10e** are shown. Lines were derived from a weighted least-squares analysis of the data points.

View Article Online
DOI: 10.1039/C6MD00586A

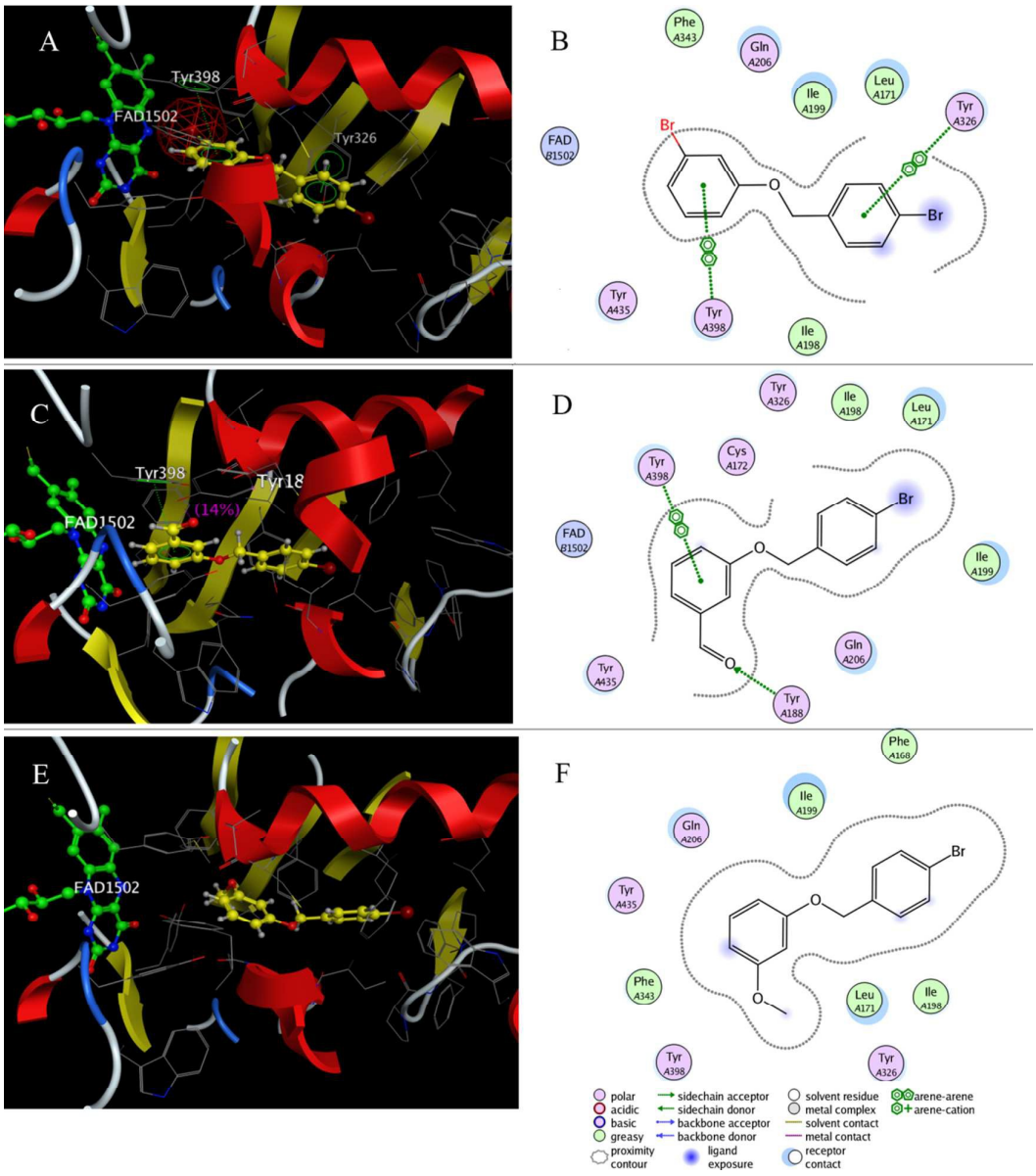

Figure 5. (A) 3D docking model of compound **9e** with *h*MAO-B. Atom colors: yellow-carbon atoms of compound **9e**, gray-carbon atoms of residues of *h*MAO-B, dark blue-nitrogen atoms, red-oxygen atoms. The dashed lines represent the interactions between the protein and the ligand. (B) 2D schematic diagram of docking model of compound **9e** with *h*MAO-B. (C) 3D docking model of compound **10e** with *h*MAO-B. (D) 2D schematic diagram of docking model of compound **10e** with *h*MAO-B. (E) 3D docking model of compound **11e** with *h*MAO-B. (F) 2D schematic

View Article Online
DOI: 10.1039/C6MD00586A

diagram of docking model of compound **11e** with *h*MAO-B. The figure was prepared using the ligand interactions application in MOE. (For interpretation of the references to color in this figure legend, the reader is referred to the web version of this article.)

View Article Online
DOI: 10.1039/C6MD00586A

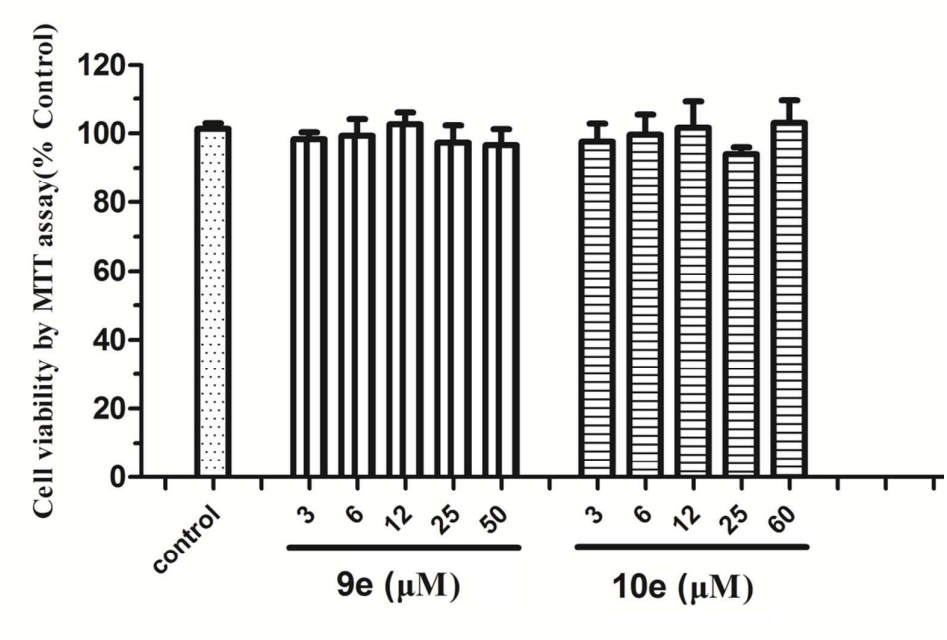

Figure 6. Effects of compounds on cell viability in SH-SY5Y cells. The cell viability was determined by the MTT assay after 48 h of incubation with various concentrations of **9e** and **10e**. The results were expressed as a percentage of control cells. Values are reported as the mean ± SD of three independent experiments.

View Article Online
DOI: 10.1039/C6MD00586A

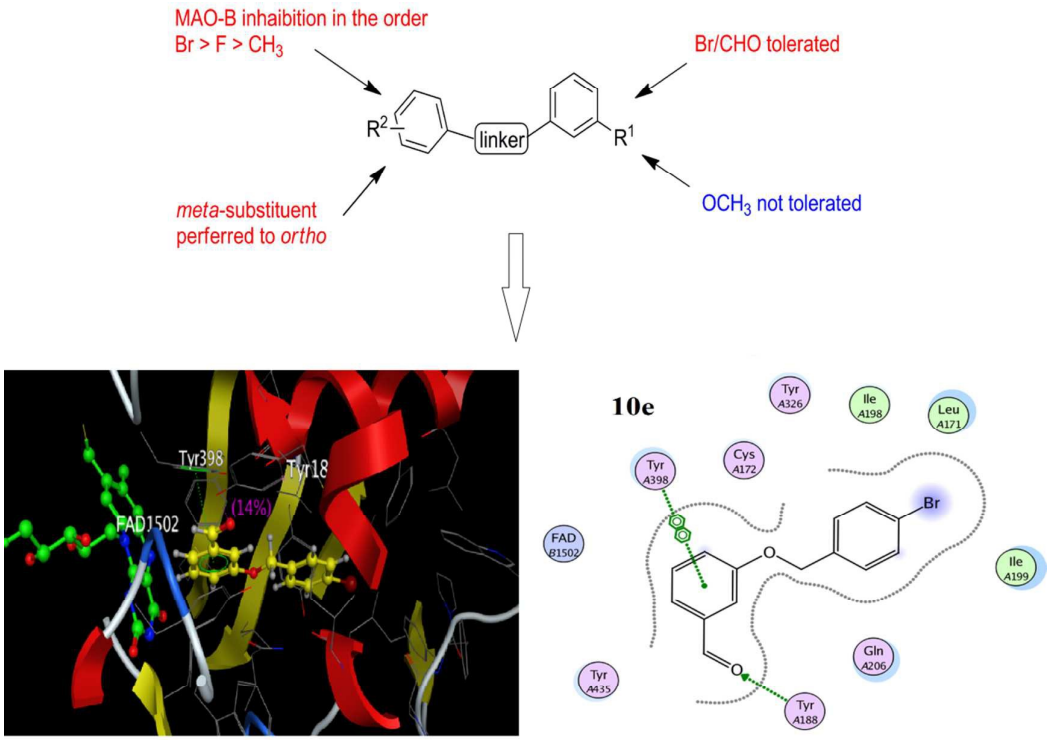

Compound **10e** IC_{50} = 0.19 μM for MAO-B inhibition